



Application of an Elongated Kelvin Model to Space Shuttle Foams

Spray-on foam insulation is applied to the exterior of the Space Shuttle's External Tank to limit propellant boil-off and to prevent ice formation. The Space Shuttle foams are rigid closed-cell polyurethane foams. The two foams used most extensively on the Space Shuttle External Tank are BX-265 and NCFI24-124. Since the catastrophic loss of the Space Shuttle Columbia, numerous studies have been conducted to mitigate the likelihood and the severity of foam shedding during the Shuttle's ascent to space. Due to the foaming and rising process, the foam microstructures are elongated in the rise direction. As a result, these two foams exhibit a non-isotropic mechanical behavior. In this paper, a detailed microstructural characterization of the two foams is presented. The key features of the foam cells are summarized and the average cell dimensions in the two foams are compared. Experimental studies to measure the room temperature mechanical response of the two foams in the two principal material directions (parallel to the rise and perpendicular to the rise) are also reported. The measured elastic modulus, proportional limit stress, ultimate tensile stress and the Poisson's ratios for the two foams are compared. The generalized elongated Kelvin foam model previously developed by the authors is reviewed and the equations which result from this model are presented. The resulting equations show that the ratio of the elastic modulus in the rise direction to that in the perpendicular-to-rise direction as well as the ratio of the strengths in the two material directions is only a function of the microstructural dimensions. Using the measured microstructural dimensions and the measured stiffness ratio, the foam tensile strength ratio and Poisson's ratios are predicted for both foams. The predicted tensile strength ratio is in close agreement with the measured strength ratios for both BX-265 and NCFI24-124. The comparison between the predicted Poisson's ratios and the measured values is not as favorable.



Application of an Elongated Kelvin Model to Space Shuttle Foams

*Roy M. Sullivan
Louis J. Ghosn
Bradley A. Lerch*

*Structures and Materials Division
NASA Glenn Research Center
Cleveland, OH*

**49th AIAA/ASME/ASCE/AHS/ASC Structures,
Structural Dynamics and Materials Conference**

Renaissance Schaumburg Hotel & Convention Center
Schaumburg, IL

April 7, 2008



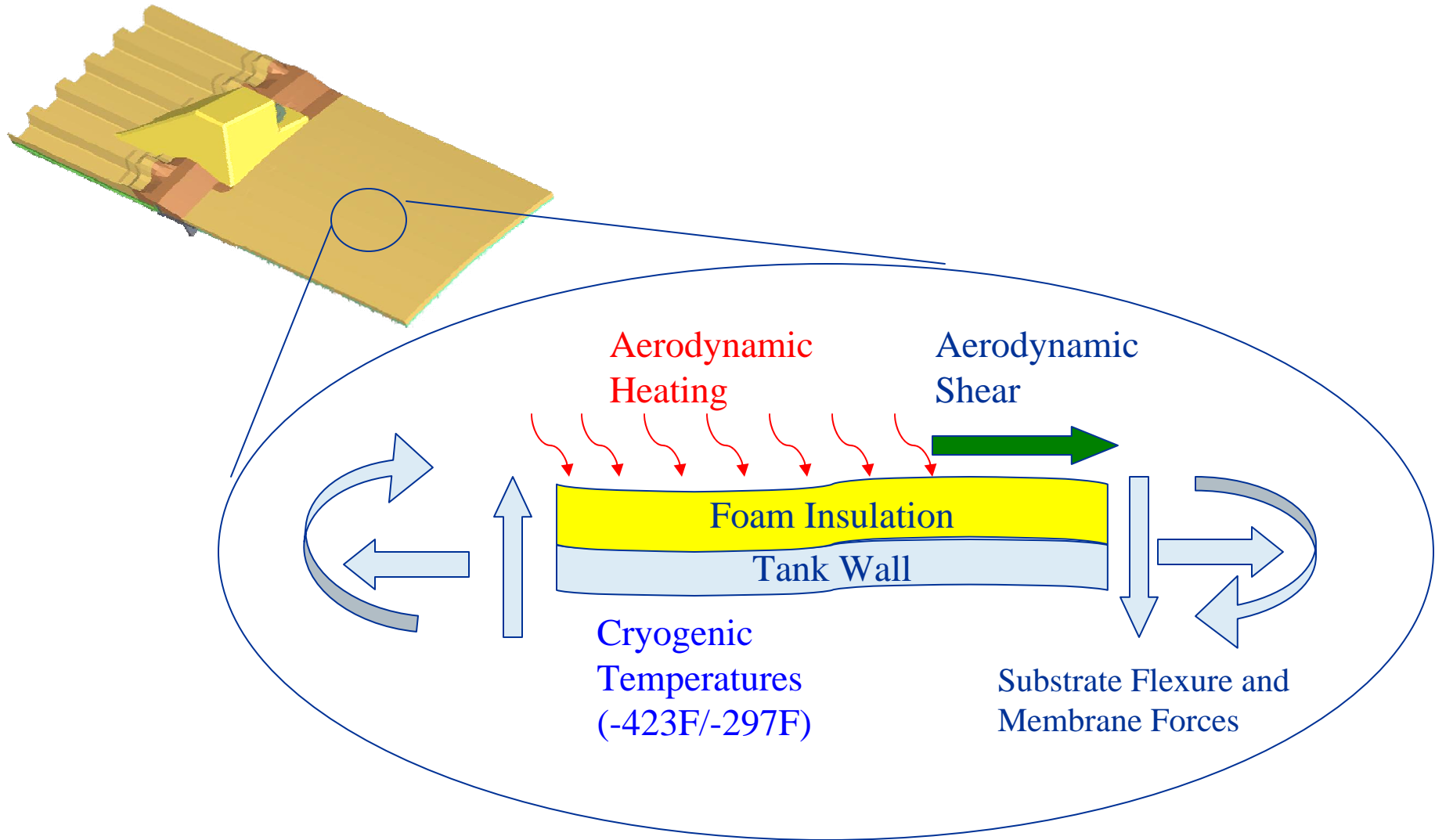
Spray-on Foam Insulation is used on the External Tank to reduce propellant boil-off and prevent ice formation on the external surfaces.

Acreage foam is NCFI24-124 (Machine sprayed)

Close-outs are hand sprayed BX-265 or PDL-1034



Typical Flight Loads on ET Foam Applications





Foam Microstructure

- 97% air; $\gamma = 0.03$
- polymeric cell walls
- due to its microstructure, material is anisotropic (possess different material properties in different directions)

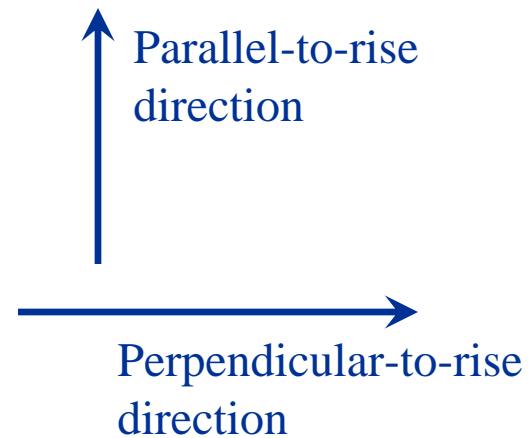
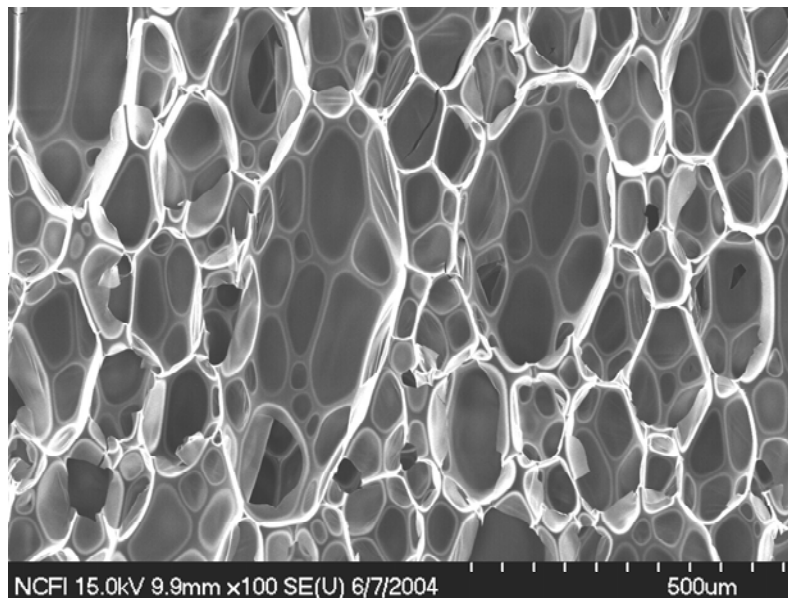
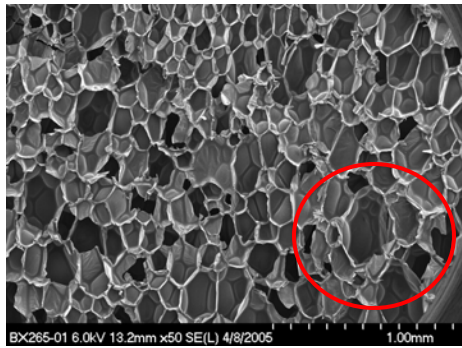


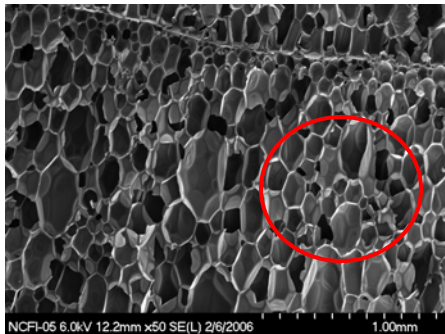
Figure 3.5 – Cell Geometry, NCFI24-124



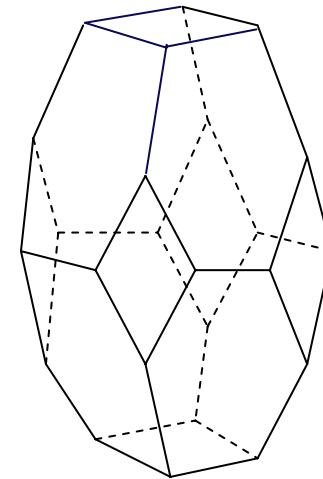
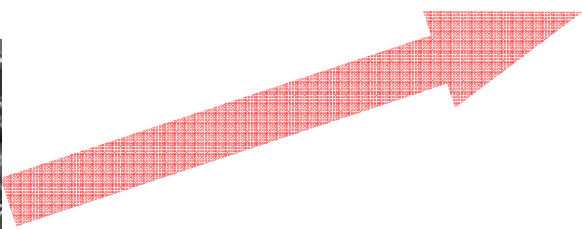
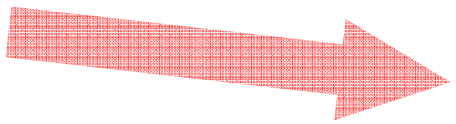
The foam microstructure can be approximated by *an elongated tetrakaidecahedron* (a fourteen-sided polyhedron)



BX-265 Average number of faces per cell: 12.4*



NCFI24-124 Average number of faces per cell: 13.7*



- 8 hexagonal faces
- 4 diamond-shaped faces
- 2 square faces
- 36 edges

* Wright L. S. and Lerch B. A., 2005. Characterization of space shuttle insulative materials, NASA/TM-2005-213596.



Some Significant Previous Studies

The tetrakaidecahedron foam model is commonly referred to as the Kelvin foam model after:

Thomson, W. (Lord Kelvin), 1887. On the division of space with minimum partitional area. *Phil. Mag.* 24, 503-514.

William Thomson (Lord Kelvin) determined that the tetrakaidecahedron (with slightly curved faces) was nature's preferred shape for soap bubbles and other foams since it is the shape that minimizes the surface area per unit volume and packs to fill space.

Equi-axial Unit Cell Models

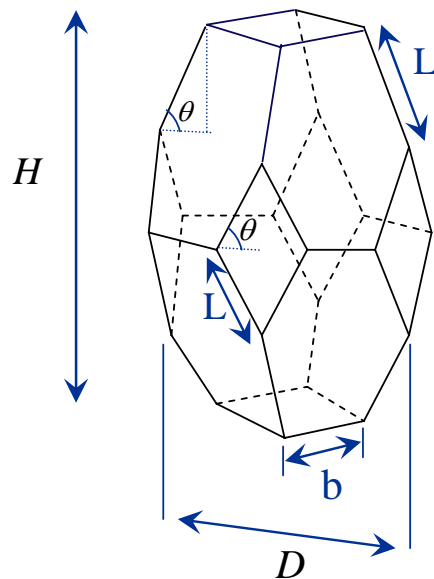
- Zhu H.X., Knott J.F. and Mills N.J., 1997. Analysis of the elastic properties of open-cell foams with tetrakaidecahedral cells. *Journal of the Mechanics and Physics of Solids* **45** (3), 319-343.
- Warren, W.E. and Kraynik, A.M., 1997. Linear elastic behavior of a low-density Kelvin foam with open cells. *Journal of Applied Mechanics* **64**, 787-794.

Elongated Unit Cell Models

- Dement'ev, A.G. and Tarakanov, O.G., 1970. Model analysis of the cellular structure of plastic foams of the polyurethane type. *Mekhanika Polimerov* **5**, 859-865. translation *Polymer Mechanics* **6**, 744-749.
- Gong, L., Kyriakides, S. and Triantafyllidis, N., 2005. On the stability of Kelvin cell foams under compressive loads. *Journal of the Mechanics and Physics of Solids* **53**, 771-794.
- Ridha, M., Shim, V.P.W. and Yang, L.M., 2006. An elongated tetrakaidecahedral cell model for fracture in rigid polyurethane foam. *Key Engineering Materials* **306-308**, 43-48.



The size and shape of an elongated tetrakaidecahedron are uniquely defined by specifying *three* independent dimensions.



$$H = 4L \sin \theta$$

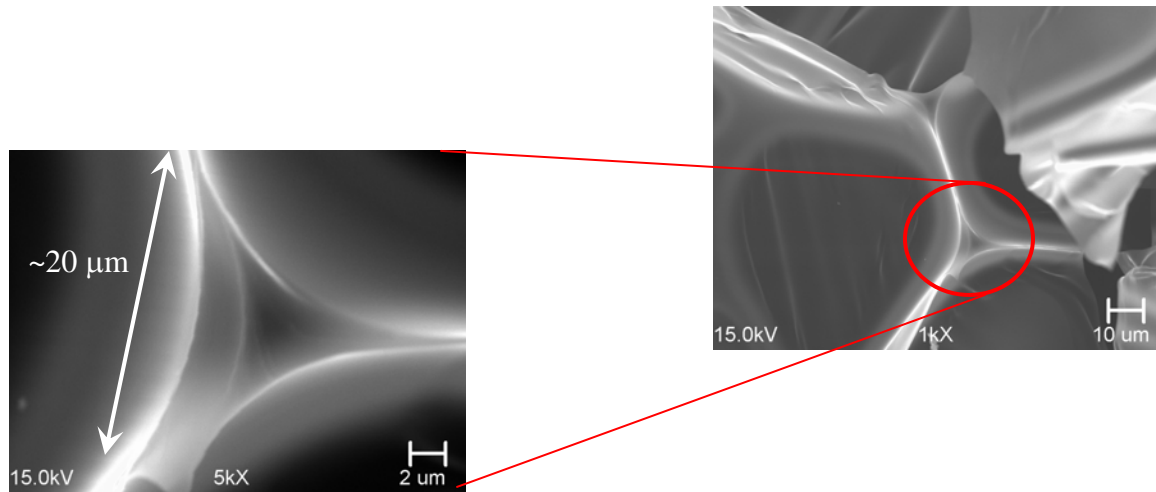
$$D = 2L \cos \theta + \sqrt{2}b$$

Aspect Ratio of Unit Cell

$$R = \frac{H}{D} = \frac{4L \sin \theta}{2L \cos \theta + \sqrt{2}b}$$



The majority of the solid mass resides in the cell edges (where the faces come together).



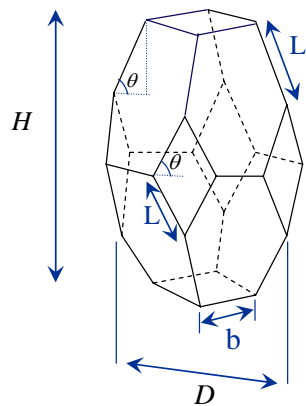
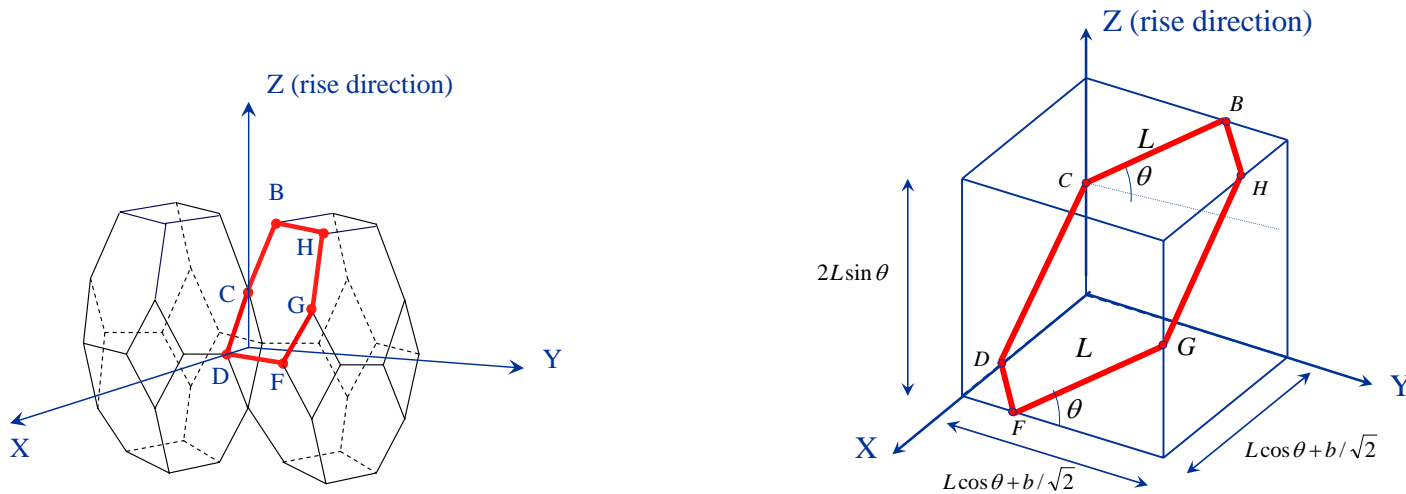
Face thickness in the middle of the faces
~ 0.1 μm to 1.0 μm

Simplifying Assumptions:

- 1) The structural rigidity of the cell faces is assumed to contribute little to the foam mechanical behavior.
- 2) The mass of the cell faces are only a small fraction of the total solid mass.



The mechanical behavior can be accurately modeled by considering the deformation of the cell edges only. The cell edges are assumed to act like struts possessing axial and flexural rigidity.

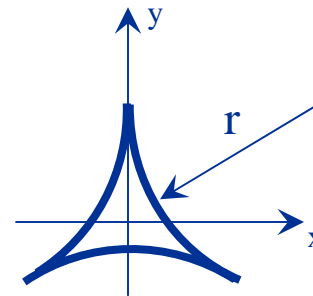
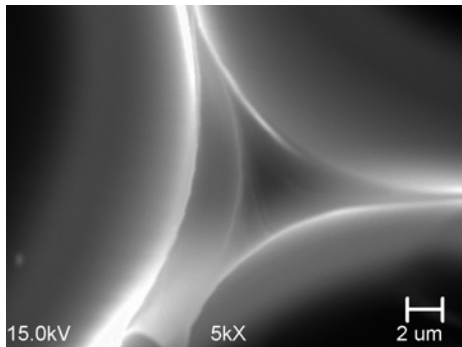


Relative Density

$$\gamma = \frac{\rho}{\rho_s} = \frac{V_{solid}}{V_{total}} = \frac{8A(2L+b)}{HD^2} = \frac{2A(2L+b)}{L \sin \theta (2L \cos \theta + \sqrt{2}b)^2}$$



Cell edge cross-sections are approximated as three-cusp hypocycloids (Plateau Borders)



Cross-section properties

I_x, I_y bending moments of inertia
 A Cross-sectional area
 S_x, S_y Section moduli

are a function of the cross-section radius only.

$$A = (\sqrt{3} - \pi/2)r^2$$

$$I_x = I_y = (20\sqrt{3} - 11\pi)r^4 / 24$$

$$S_x = (60 - 11\sqrt{3}\pi)r^3 / 24$$

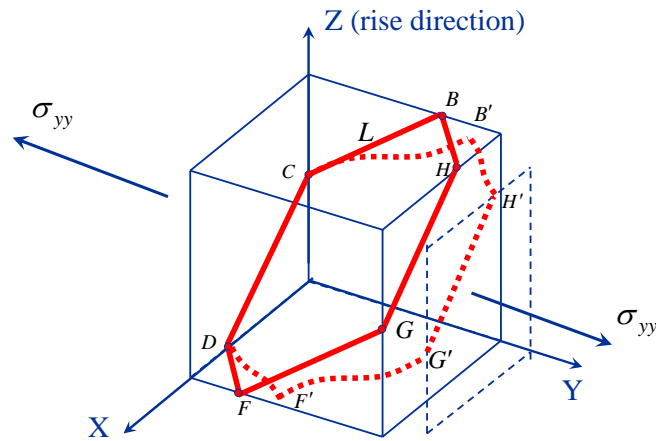
$$S_y = (20\sqrt{3} - 11\pi)r^3 / 12$$

Thus, four microstructural dimensions are required:

3 to define the unit cell + 1 to specify the edge cross-section dimension



Careful consideration of the unit cell deformation leads to convenient algebraic equations for the Young's modulus, Poisson's ratio and strengths in the principal material directions.



Poisson's ratios:

$$\nu_{xy} = \nu_{yx} = \frac{b(Ab^2 - 12I)}{12I(2L \cos^2 \theta + b) + A(2L^3 \sin^2 \theta + b^3)}$$

$$\nu_{xz} = \nu_{yz} = \frac{(AL^2 - 12I)(2L \cos \theta + \sqrt{2}b) \cos \theta}{2[12I(2L \cos^2 \theta + b) + A(2L^3 \sin^2 \theta + b^3)]}$$

$$\nu_{zx} = \nu_{zy} = \frac{\sqrt{2}L^2(AL^2 - 12I) \cos \theta \sin^2 \theta}{[12IL \sin^2 \theta + AL^3 \cos^2 \theta][\sqrt{2}L \cos \theta + b]}$$

Young's moduli:

$$E_x = E_y = \frac{12EI}{L \sin \theta \left[2L^3 \sin^2 \theta + b^3 + \frac{12I}{A} (2L \cos^2 \theta + b) \right]}$$

$$E_z = \frac{24EI \sin \theta}{L^2 \left[\cos^2 \theta + \frac{12I \sin^2 \theta}{AL^2} \right] [\sqrt{2}L \cos \theta + b]^2}$$

Strengths:

based on peak stress in any edge reaching solid material strength σ^s

$$\sigma_{xx}^s = \sigma_{yy}^s = \frac{\sigma^s}{\left[\frac{L \cos \theta \sin \theta}{A} + \frac{L^2 \sin^2 \theta}{2S_x^L} \right] [2L \cos \theta + \sqrt{2}b]}$$

Failure of the L-length edges

$$\sigma_{xx}^s = \sigma_{yy}^s = \frac{\sigma^s}{\left[\frac{L \sin \theta}{\sqrt{2}A} + \frac{Lb \sin \theta}{2\sqrt{2}S_z^b} \right] [2L \cos \theta + \sqrt{2}b]}$$

Failure of the b-length edges

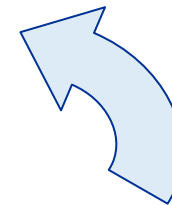
$$\sigma_{zz}^s = \frac{\sigma^s}{\left[\frac{\sin \theta}{2A} + \frac{L \cos \theta}{4S_x^L} \right] [\sqrt{2}L \cos \theta + b]^2}$$



The ratio of the rise direction modulus to the normal-to-rise direction modulus and the ratio of the strengths are indicative of the amount of elongation.

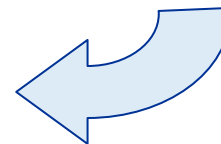
Stiffness Ratio

$$R_E = \frac{E_z}{E_x} = \frac{E_z}{E_y} = \frac{R^2}{4} \frac{\left[2 \sin^2 \theta + (b/L)^3 + \frac{12I}{AL^2} (2 \cos^2 \theta + b/L) \right]}{\left[\cos^2 \theta + \frac{12I}{AL^2} \sin^2 \theta \right]}$$



Strength Ratio

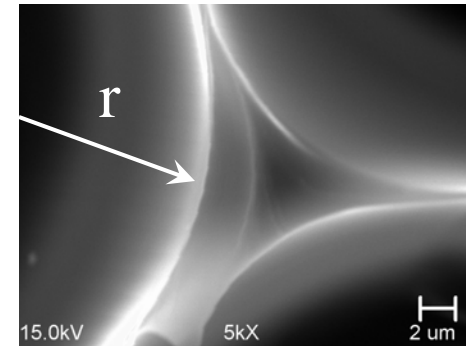
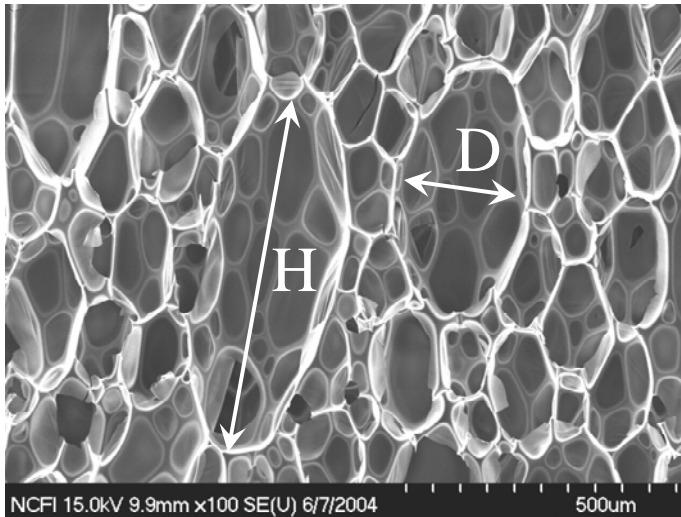
$$R_\sigma = \frac{\sigma_{zz}^s}{\sigma_{xx}^s} = \frac{\sigma_{zz}^s}{\sigma_{yy}^s} = R \frac{2S_x^L \cos \theta + AL \sin \theta}{2S_x^L \sin \theta + AL \cos \theta}$$



*Doesn't involve the properties of the solid material.
Only a function of the unit cell dimensions and
the edge cross-section dimension.*



Microstructural Characterization



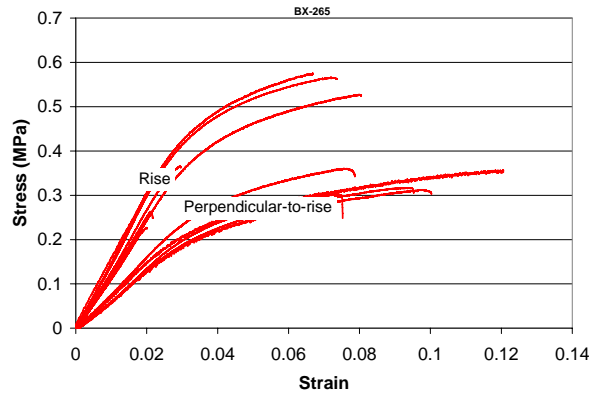
	Cell Height H		Cell Width D		Edge Cross-section Radius r		Aspect Ratio $R = H / D$
	Avg., μm	n	Avg., μm	n	Avg., μm	n	
BX-265	193	100	136	100	NA*		1.42
NCFI24-124	248	100	142	100	26.0	27	1.75

* Data not available

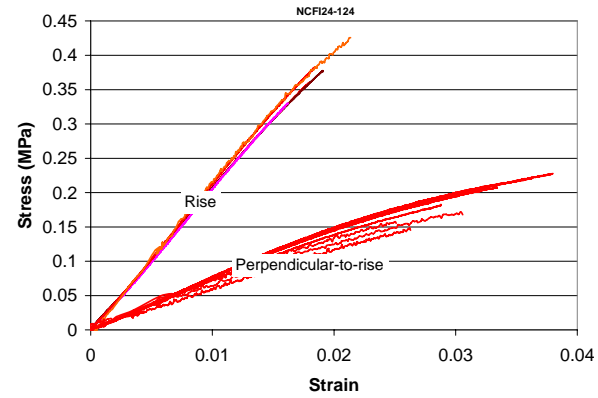


Mechanical Testing

BX-265



NCFI24-124



Average Properties

	Initial Modulus (MPa)		Proportional Limit (kPa)		Ult. Tensile Strength (kPa)		Ratios		
	Rise	Normal-to-rise	Rise	Normal-to-rise	Rise	Normal-to-rise	Stiffness	Proportional Limit	Ultimate Tensile Strength
BX-265	13.53	7.03	315.4	173.5	555.8	319.4	1.92	1.82	1.74
NCFI24-124	20.80	7.07	248.1	110.3	375.4	188.2	2.94	2.25	1.99



Mechanical Testing

Poisson's Ratios

Average Density

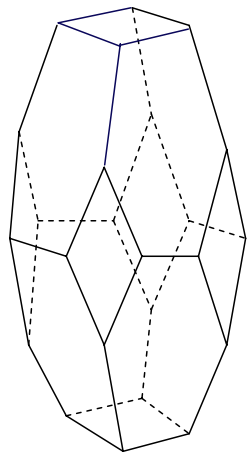
	Average Density (g/cc)	Relative Density*
BX-265	0.0369	0.031
NCFI24-124	0.0373	0.031

* Calculated assuming density of polymer is 1.2 g/cc.

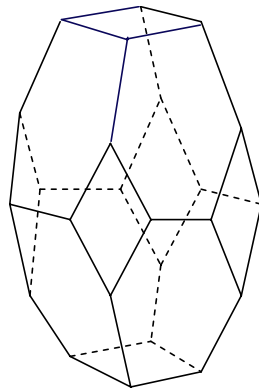
		Avg. Measured Poisson's Ratio	Standard Deviation
BX-265	ν_{xy}	0.355	0.06
	ν_{xz}	0.273	0.0007
	ν_{zx}	0.536 0.675	0.29 0.17
NCFI24-124	ν_{xy}	0.382	0.14
	ν_{xz}	0.183	0.04
	ν_{zx}	0.641	0.10



The shape is defined by the aspect ratio $R = \frac{H}{D}$
 and the shape parameter $Q = \frac{b}{L \cos \theta}$

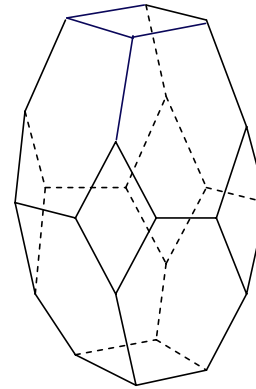


$$R = R_A$$

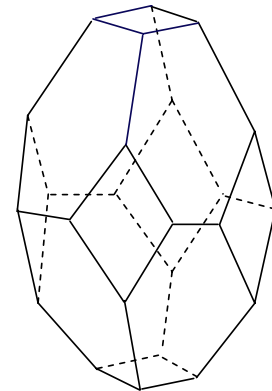


$$R = R_B$$

$$R_A > R_B$$



$$Q = Q_A$$



$$Q = Q_B$$

$$Q_A > Q_B$$



in terms of $L, b, \theta, I/A$

$$R_E = \left(\frac{4L \sin \theta}{2L \cos \theta + \sqrt{2}b} \right)^2 \frac{\left[2 \sin^2 \theta + (b/L)^3 + \frac{12I}{AL^2} (2 \cos^2 \theta + b/L) \right]}{4 \left[\cos^2 \theta + \frac{12I}{AL^2} \sin^2 \theta \right]}$$

$$R_\sigma = \left(\frac{4L \sin \theta}{2L \cos \theta + \sqrt{2}b} \right) \frac{\left(\frac{2S_x^L}{AL} \cos \theta + \sin \theta \right)}{\left(\frac{2S_x^L}{AL} \sin \theta + \cos \theta \right)}$$

$$R = \frac{4L \sin \theta}{2L \cos \theta + \sqrt{2}b} \quad Q = \frac{b}{L \cos \theta} \quad \gamma = \frac{2A(2L+b)}{L \sin \theta (2L \cos \theta + \sqrt{2}b)^2}$$

in terms of R, Q, γ

$$R_E = \frac{R^2}{4} \left[\frac{\left(2\tilde{Q}^2 R^2 + \frac{64Q^3}{\sqrt{16 + \tilde{Q}^2 R^2}} \right) C_1 + \frac{8RC_2 \tilde{Q}^3 (32 + 4Q\sqrt{16 + \tilde{Q}^2 R^2})}{(4Q + 2\sqrt{16 + \tilde{Q}^2 R^2})(16 + \tilde{Q}^2 R^2)} \gamma}{16C_1 + \frac{8R^3 C_2 \tilde{Q}^5}{(4Q + 2\sqrt{16 + \tilde{Q}^2 R^2})(16 + \tilde{Q}^2 R^2)} \gamma} \right]$$

$$R_\sigma = R \left[\frac{\sqrt{C_1} \tilde{Q} R + \frac{16\sqrt{2}C_3 \tilde{Q}^{1.5} R^{0.5} \gamma^{0.5}}{(4Q + 2\sqrt{16 + \tilde{Q}^2 R^2})^{0.5} (16 + \tilde{Q}^2 R^2)^{0.5}}}{4\sqrt{C_1} + \frac{4\sqrt{2}C_3 \tilde{Q}^{2.5} R^{1.5} \gamma^{0.5}}{(4Q + 2\sqrt{16 + \tilde{Q}^2 R^2})^{0.5} (16 + \tilde{Q}^2 R^2)^{0.5}}} \right]$$

$$\tilde{Q} = 2 + \sqrt{2}Q$$

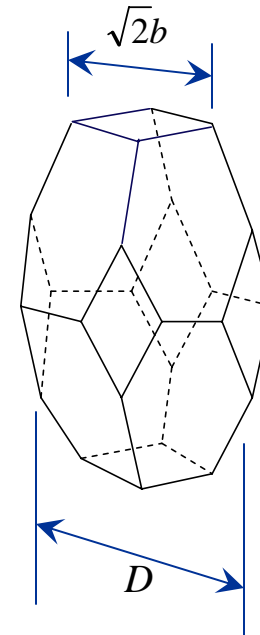


Previous research studies using the elongated Kelvin model set an artificial restriction on the unit cell shape,

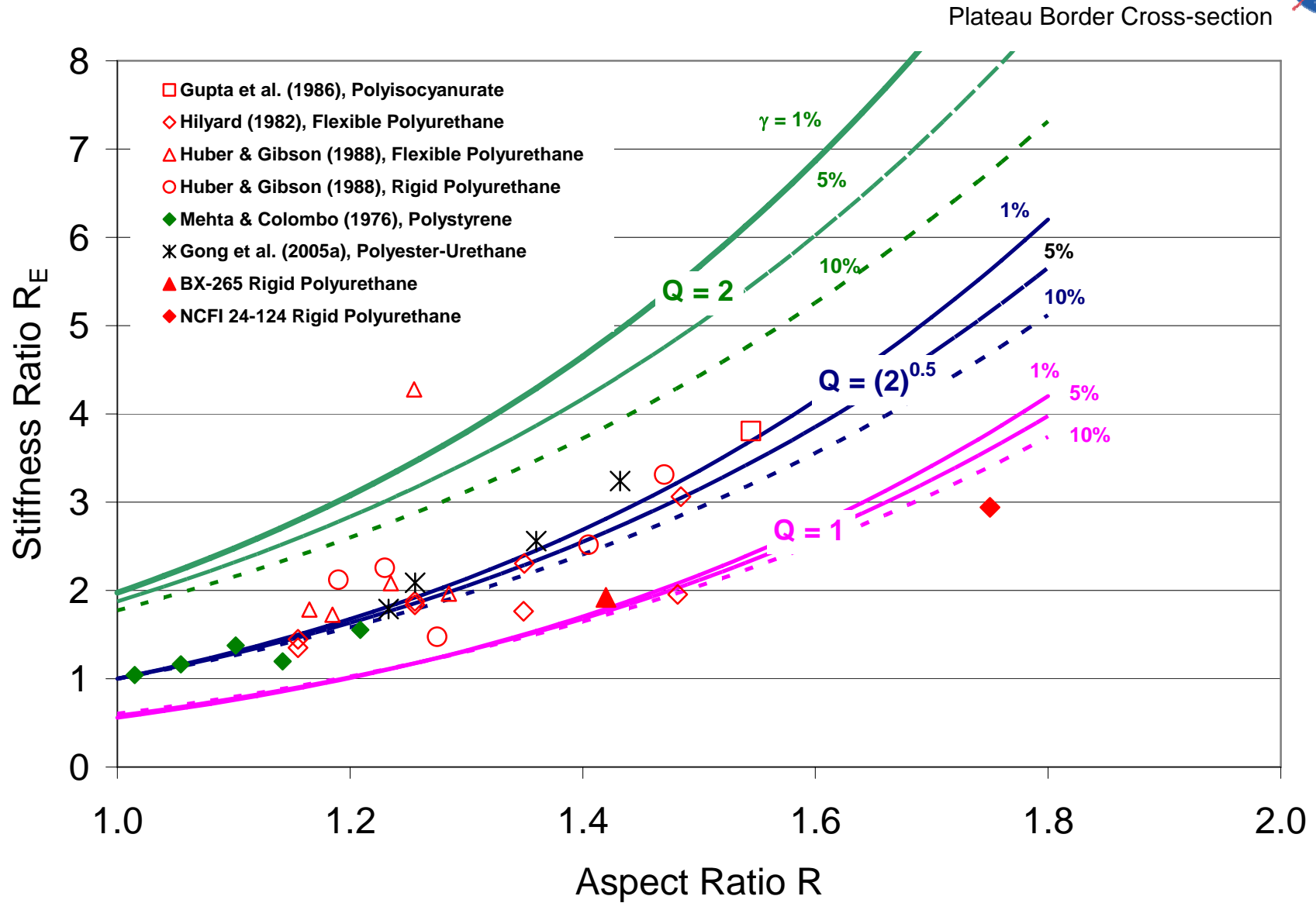
$$b/L = \sqrt{2} \cos \theta \quad \longrightarrow \quad Q = \sqrt{2}$$

which is equivalent to assuming that $D = 2\sqrt{2}b$

*This reduces the number of unit cell dimensions required to exercise the theory and apply the equations by one. The unit cell shape is now described by specifying only **two** dimensions.*

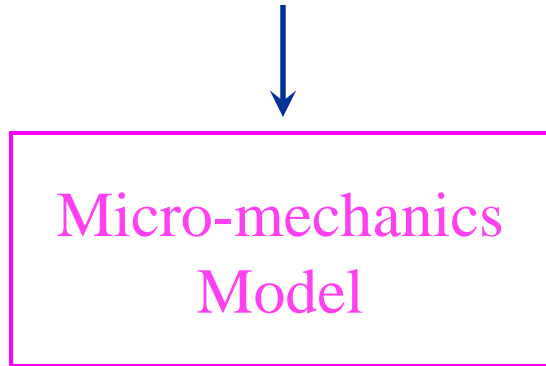


However, this restriction on the unit cell geometry seems arbitrary and it reduces the generality of the model and limits its applicability to a narrower range of foams.





	$D(\mu m)$	R	γ	R_E
BX-265	136	1.42	0.031	1.9
NCFI24-124	142	1.75	0.031	2.9



$$b = \frac{D}{\sqrt{2} + \frac{2}{Q}}$$

$$L = \frac{b\sqrt{16 + (2 + \sqrt{2}Q)^2 R^2}}{4Q}$$

$$r = \sqrt{\frac{\gamma RD^3}{C_1(16L + 8b)}}$$

	BX-265		NCFI24-124	
	Predicted	Measured	Predicted	Measured
Q	1.0747	--	0.7765	--
R_σ	1.75	1.82 PL 1.74 ult.	2.34	2.25 PL 1.99 ult.
$b (\mu m)$	41.5	35.0*	35.6	NA
$L (\mu m)$	61.8	63.0*	77.2	NA
$r (\mu m)$	22.8	18.0*	25.2	26.0
v_{xy}	.177	.355 ± 0.06	.060	.382 ± 0.14
v_{xz}	.422	.273 ± 0.0007	.373	.183 ± 0.04
v_{zx}	.811	.536 ± 0.29 .675 ± 0.17	1.097	.641 ± 0.10

* Measurements from another block of BX-265.
NA Data not available.



Finite Element Analysis of an Elongated Kelvin Model

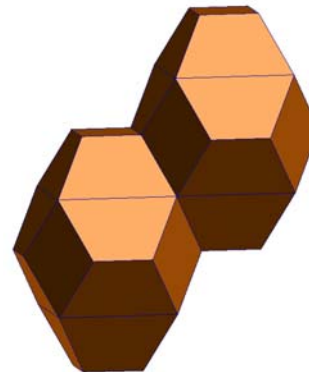
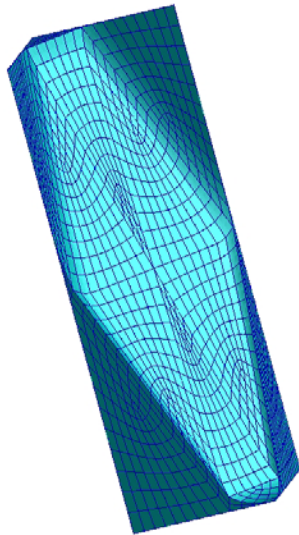
Unit cell dimensions

- $R = 1.72$
- $D = 144 \mu m$
- $b = 24 \mu m$
- $L = 90.6 \mu m$
- $r = 20.2 \mu m$

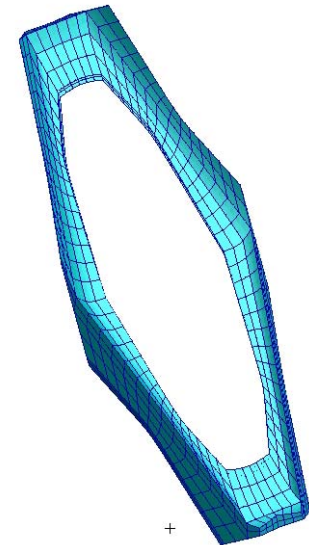
Solid Properties

- $E = 2GPa$
- $\nu = 0.3$

Closed Cell



Open Cell



	Closed cell	Open cell
γ	1.62%	1.24%
ν_{xy}	0.621	0.024
ν_{xz}	0.120	0.230
ν_{zx}	0.256	1.727

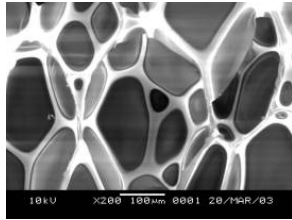


Summary and Conclusions

- Model was successful in predicting the measured strength ratios and edge cross-section radii using measured average cell height, cell width, relative density and stiffness ratios as input.
- Prediction of Poisson's ratios was not as successful.
- Shuttle foams have a microstructure such that $Q \neq \sqrt{2}$, so a micromechanics model derived from a general elongated Kelvin unit cell is needed.
- Future work should include performing finite element analysis of BX-265 and NCFI24-124 unit cells with faces included and predict Poisson's ratios.



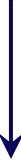
Backup Slides



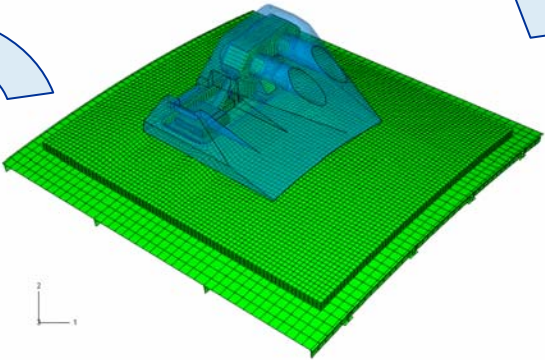
*Description of
Foam Microstructure*



**Micro-mechanics
Model**



Foam Elastic Constants



Average Foam Stresses

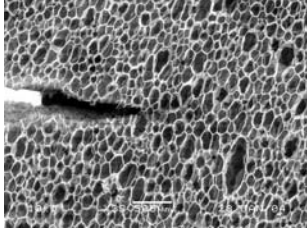
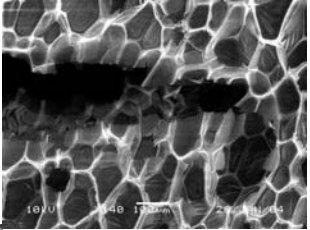
Finite Element Analysis



**Micro-mechanics
Model**



*Edge (Strut) Stresses
and Failure Initiation*





Manual Spray Close-outs of BX-265

Intertank Flanges



Protrusion Air Load (PAL) Ramp

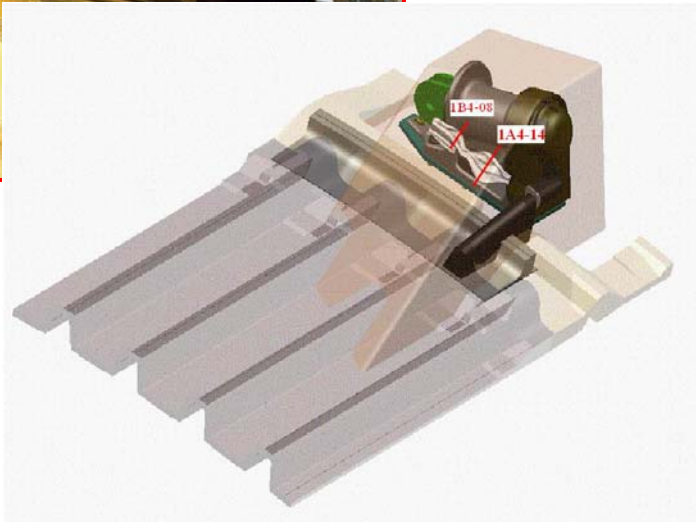
Redesign eliminated the LOx and LH₂ PAL Ramps





Bipod Fitting and Ramp Closeout

BX-265

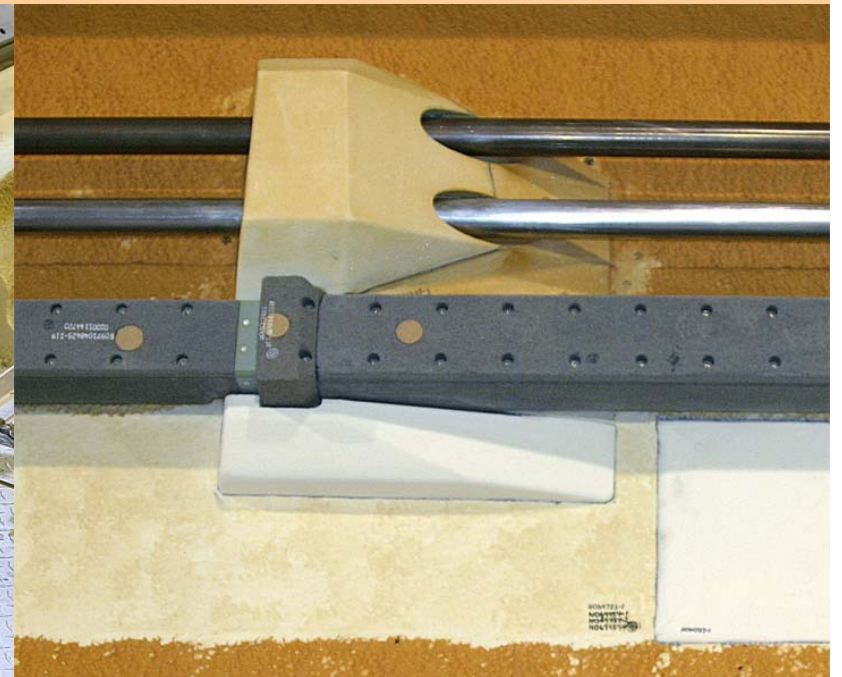
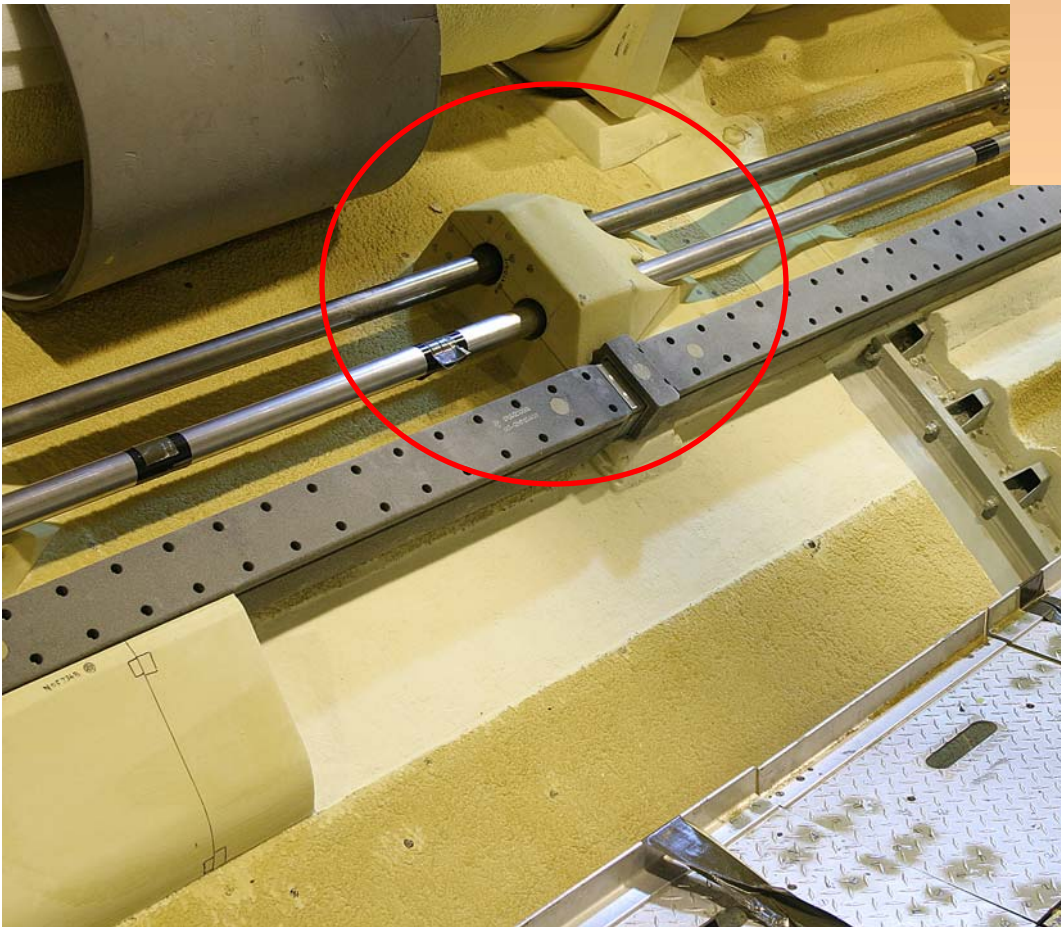
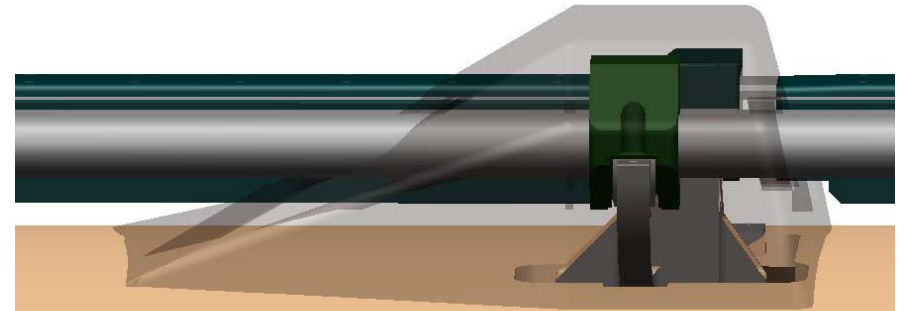


Current design

Ice Frost Ramps

PDL-1034

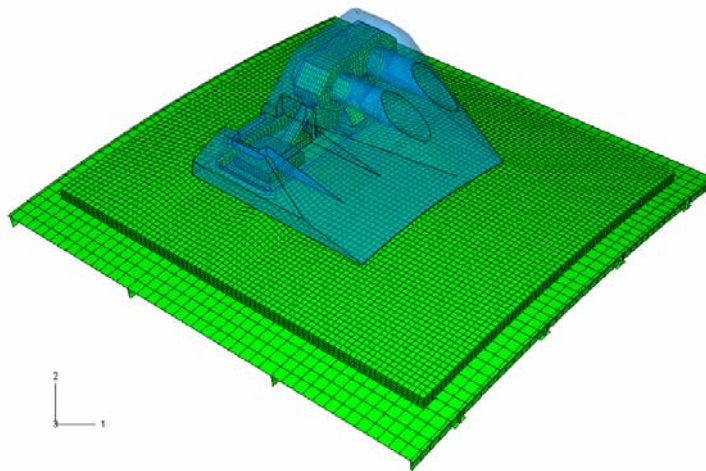
Cover the pressurization line and cable tray support fittings to prevent ice formation.



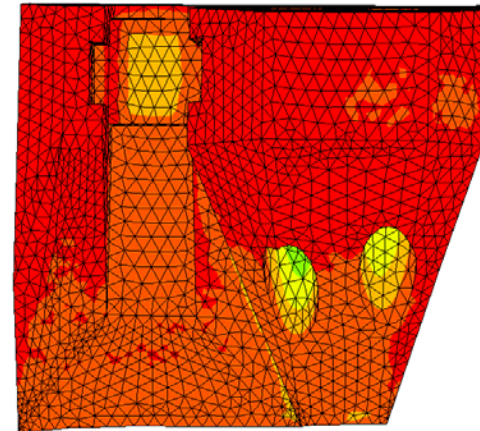




Structural Analysis of the Foam Applications under launch loads and environments is performed by Finite Element Analysis



Pa	PSI
111300	16.142
101600	14.735
91840	13.320
82090	11.906
72350	10.493
62610	9.080
52870	7.668
43120	6.254
33380	4.841
23640	3.429
13890	2.015
4152	0.602
-5591	-0.811



Finite element analysis treats the foam material as a homogeneous, temperature dependant and orthotropic material

- elastic constants and strengths obtained during material characterization testing*
- the effect of a varying microstructure on the foam structural integrity is neglected*

Analyses are not used for flight qualification, but as a tool to study possible foam shedding mechanisms and to guide proposed design changes.